Jurnal
Teknologi

Full Paper

AUTOMATED DEFORM DETECTION ON AUTOMOTIVE BODY PANELS USING GRADIENT FILTERING AND FUZZY C-MEAN SEGMENTATION

M. Z. B. Edris*, Z. Zakaria, M. S. I. M. Zin, M. S. Jawad

Centre for Telecommunication Research and Innovation (CeTRI), Faculty of Electronics and Computer Engineering, Universiti Teknikal Malaysia Melaka (UTeM), 76100 Durian Tunggal, Melaka, Malaysia

Article history
Received
10 June 2015
Received in revised form
25 September 2015
Accepted
30 December 2015

*Corresponding author
zuhairbolqiah@gmail.com

Graphical abstract

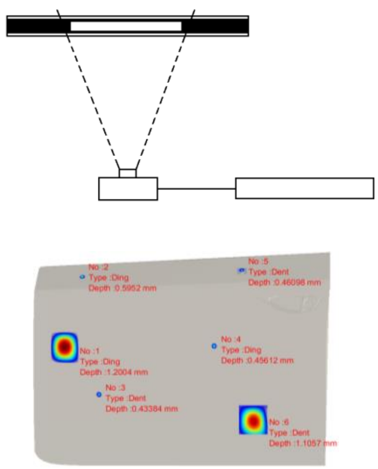

Abstract

Automatic deform detection on automotive body panel is challenging owing to its localization on a large surface, variation in appearance, and their rare occurrences. It is difficult to detect these deforms either by original models or by small-sample statistics using a single threshold. As a consequence, this problem is focussed to derive a lot of good-quality deform detected from the surface images. These detections should discriminate the various surface deforms when fed to suitable image processing algorithms. This paper used gradient filtering and background illumination correction to identify the deform area. An algorithm to segment the deform area has been developed. It segments the deformation by using Fuzzy C-Means (FCM) segmentation. The algorithm is being test on three samples which are car door model, curve and flat surface with two types of deformations which is ding and dent deformations that occur on the surface.

Keywords: Deformation Detection, Segmentation, Gradient Filtering, Fuzzy C-Means thresholding, Otsu thresholding.

1.0 INTRODUCTION

Quality control is an important aspect of all industrial production. Nowadays, many automated system is developed to reduce costs and improve the quality of the product. However, at the last point of production, quality assurance with regard to surface deforms is partly automated and largely caused by manual inspection. Traditionally, human labour is used to inspect the manufactured automotive body panels. The worldwide economic evolution has gradually led steel production industries to increase its production rate, ensuring simultaneously stringent limit on the quality of products.

The automated inspection is necessary in manufacturing industries to improve the quality of production as to replace human intervention because of hazardous environment. This will make it easier to identify the deformation and notify immediately after manufacturing process has been finished. This receives an obvious benefit in terms of quality assurance. The surface deforms often arise as a result of systematic process problems, such as (partially) damaged machinery or metallurgical drift. Thus, the early detection of deforms can also have a direct cost benefit in conditions of saving of time as well as to prevent rejection from being generated in large quantities, in downstream [1].

In the past researches, many methods of defect or deformation detection are being proposed. Advanced surface shape analysis techniques must be performed to determine the locations of probable deformations. Given that the three-dimensional data can be converted from a range image to a two-dimensional image where each pixel value represents the depth of that point on the object from the viewpoint, features can be extracted and images can be segmented using traditional two-dimensional image processing techniques [2].

The most critical component of a surface deformation detection system is a surface analysis to locate the deformations in query. In the current context, no ideal model of the automotive part is supplied, so the algorithm has no a priori knowledge of what the surface should look like without deformations. On that point are certain major difficulties in the deform detection of automotive body panels. The deformations of interest are dings and dents, where dings are surface deformations which protrude from the surface and dents are depressions into the surface. This paper focuses on deformation detection when no ideal model of the automotive part is provided, similar to an approach which is alluded to by [3] and explored by [4]. Since there is no CAD model of a masterwork to compare the measured model to, the deformation detection must be performed without knowledge of the expected surface and involves certain premises to be drawn based on common characteristics of surface deformations compared to the characteristics of a un-deformed surface. However, not all characteristics can be assumed, known, or easily defined. Then close to basic parameters need to be set by the operator to provide the system with a minimal knowledge of the approximate size or plate of the distortions that the manufacturer wants to detect and eliminate from its products. This is not unrealistic, as the operator generally has a clear idea of the approximate range of sizes for the deformations to be found [2].

In this paper, an algorithm is being develop to detect the deformation occur on the automotive body panels where it is to segment the deform area. The gradient filtering and background removal methods are proposed to determine the uneven contour on the surface as pre-processing stage. The thresholding method is used to segment the deformed area. The Fuzzy C-Means (FCM) and Otsu's tresholding are being used to determine which methods have better performance. The evaluations of performance are based on their accuracy of segmentation, false positive rate and false negative rate and sensitivity.

2.0 PRE-PROCESSING

Morphological on gray-scaled image is used throughout this part. The nature of the morphological operations gives rise to a set of parameters, which must be set in accordance to a definition of what, is the non-deform surface look like. Thus these parameters have been set experimentally from the model set, while considering their relation to adequate physical measures relevant to the problem.

2.1 Gradient Filtering

Metal plane has flat surface, but it can be formed into various shapes. Nevertheless, the deformation may occur in the certain surface region, the gradient of the surface is being identified by working out the image gradient using image first order derivatives. The aim of this first order derivative of the surface is to rent out the gradient magnitude of the aerofoil. The magnitude is shown the information of grey scale intensity gradient. If the intensity of one pixel to adjacent pixel is changed substantial, the magnitude is high while if it's slightly changes of grey scale intensity the gradient is low.

To achieve this method, the first order derivative is applied into the matrix or image. The resulting data that will produces is the gradient value between two adjacent pixels according into their pixel value. The first order derivatives of an image can be done by convoluting image to a filter. There are two directions of gradient that can be calculated which are the x and y direction. The gradient is a measure of modification in a function, and an image can be considered to be an array of samples of some continuous function of image intensity. The slope is the two-dimensional equivalent of the first derivative and is set as the vector. The gradient of an image is can be given into the formula [5]:

$$\nabla f = \begin{bmatrix} g_x \\ g_y \end{bmatrix} = \begin{bmatrix} \frac{\delta f}{\delta x} \\ \frac{\delta f}{\delta y} \end{bmatrix} \tag{1}$$

Where $\frac{\delta f}{\delta x}$ is gradient in x direction, whereas $\frac{\delta f}{\delta y}$ is gradient in y direction. There are two important attributes associated with the gradient which is the vector ∇f points in the direction of the maximum rate of increase of the function ∇f and the magnitude of the gradient, which is given by:

$$\nabla f = \sqrt{g_x^2 + g_y^2} \tag{2}$$

For array matrix, below equation is the derivatives of approximated by differences. The simplest gradient approximation is:

$$g_x \cong f[i,j+1] - f[i,j] \quad (3)$$

$$g_y \cong f[i,j] - f[i+1,j] \quad (4)$$

Therefore, the gradient filtering is being apply to the normalize image result of the surface gradient filtering. The convolution of the image and filter has been done. There are two types of filter being used which is given array below:

$$\frac{\delta}{\delta x} = \begin{bmatrix} -1 & 0 \\ 0 & 1 \end{bmatrix}, \quad \frac{\delta}{\delta y} = \begin{bmatrix} 0 & -1 \\ 1 & 0 \end{bmatrix} \quad (5)$$

and

$$\frac{\delta}{\delta x} = [1 \quad -1], \quad \frac{\delta}{\delta y} = \begin{bmatrix} 1 \\ -1 \end{bmatrix} \quad (6)$$

Then, the convolution between image f with $g_x$and g_y is take place where:

$$f_x = f \otimes \frac{\delta}{\delta x} \quad (7)$$

$$f_y = f \otimes \frac{\delta}{\delta y} \quad (8)$$

The image is apply to this four filters and the result of four image will be add in each result for example, we consider for first filter is denote as f_{x1} and f_{y1} and result for another filter is denote as f_{x2} and f_{y2} , the sum of gradient is being calculated as:

$$f = |f_{x1}| + |f_{y1}| + |f_{x2}| + |f_{y2}| \quad (9)$$

Therefore, the result after the four result has being add to each other, the low value of magnitude is the value that the gradient of each adjacent pixel is low while the high magnitude value is the sudden changes of each adjacent pixels.

2.2 Correcting Non-Uniform Illumination

The surface of body panels is not in flat shape or surface so the surface deforms detection will be difficult to implement. By correcting the non-uniform illumination, the curve shaped of the body panel will be flatted. To correct the non-uniform illumination, the morphological process of the grey-scaled is implemented by using concept of erosion and dilation.

2.2.1 Erosion and Dilation

Erosion is the techniques that remove the boundary regions of the foreground pixel. Therefore, the image pixel will be shrinking. Thus, areas of foreground pixels shrink in size, and holes within those areas become larger [6].

For example, the erosion of I by a flat structuring element H at any location (x, y) is defined as the minimum value of the image in the region coincident with H when the origin of H is at(x, y). Therefore, the erosion at (x, y) of an image I by a structuring element H is given by:

$$[I \ominus H](x, y) = \min_{(i,j)\in H} \{I(x+i, y+j)\} \quad (10)$$

Where similarly to the correlation, x and y are incremented through all values required so that the origin of H visits every pixel in I. That is, to find the erosion of $I_{(x,y)}$ by H, the origin of the structuring element can be placed at every pixel location in the image. The erosion is the minimum value of I from all values of I in the region of $I_{(x,y)}$ coincident with H [7].

The dilation of I by a flat structuring element H at any location (x, y) is defined as the maximum value of the image in the window outlined by when the origin of being at (x, y). That is:-

$$[I \oplus H](x, y) = \max_{(i,j)\in H} \{I(x-i, y-j)\} \quad (11)$$

Where $\bar{H}$ can be used as:

$$\bar{H} = H(-x, -y) \quad (12)$$

The explanation is similar to one for erosion except for using maximum instead of minimum and that the structuring element is reflected about the origin [7].

3.0 SEGMENTATION

In segmentation process, Fuzzy C-Means (FCM) and Otsu's thresholding methods are being used to automatically segment the deform area by performing clustering-based image thresholding [8] or, the reduction of a gray scaled image to a binary image.

3.1 Fuzzy C-Mean Thresholding Segmentation

The Fuzzy C-Means (FCM) method has been introduced by [9] where the membership is assigned to each data point that corresponding to each cluster center on the basis of distance between the cluster and the data point. When more the data is near to the cluster center more is its membership towards the particular cluster center. Summation of the membership of each data point should be equal to one [10]. The algorithm is based on minimization of the following objective function as shown in Equation (13) [11]:

$$j_m = \sum_{i=1}^{N} \sum_{j=1}^{C} u_{ij}^m \left\| x_i - c_j \right\|^2, 1 \le m \le \infty \quad (13)$$

Where m is any number greater than 1, N is a number of data, C is the number of clusters, u_{ij} is the degree of the membership of x_i in the cluster j, x_i is the i^{th} of d-dimensional measured data, c_j is the d-dimension center of the cluster, and $\|*\|$ is any norm expressing the similarity between any measured data and center. Fuzzy partition carried out through an iterative optimization of the objective function shown in Equation (14), with the membership u_{ij} and the cluster centers c_j by [11]:

$$u_{ij} = \frac{1}{\sum_{k=1}^{C}\left(\frac{\|x_i - c_j\|}{\|x_i - c_k\|}\right)^{\frac{2}{m-1}}} \tag{14}$$

Where $\|x_i - c_j\|$ is the distance from point i to current cluster center j, $\|x_i - c_k\|$ is the distance from point i to the cluster center k.

$$c_j = \frac{\sum_{i=1}^{N} u_{ij}^{m} \cdot x_i}{\sum_{i=1}^{N} u_{ij}^{m}} \tag{15}$$

The iteration will stop when:

$$max_{ij}\left\{\left|u_{ij}^{k+1} - u_{ij}^{(k)}\right|\right\} < \varepsilon \tag{16}$$

Where ε is a termination criterion between 0 and 1, whereas k is the iteration step. This procedure converges to a local minimum or a saddle point j_m.

The algorithm can be ended in two ways which are by computing the fuzzy membership function and by calculating the cluster centers value. The cluster centers are initialized with random values ranged. It is between maximum and minimum normalized gray level. Due to the unknown variables of the cluster centers and the fuzzy membership cannot be computed directly. When the difference between two clusters at two successive iterations is less than ε, the stopping criterion for Fuzzy C-Means (FCM) is met.

3.2 Otsu's Thresholding Segmentation

While considering normalized gray-scale intensity as a function, f and containing N pixels with gray levels value from 0 to 1. The number of pixels with gray level i is denoted by f_i, so the probability of gray level i in an image is calculated as show in equation (17) [12]:

$$P_i = \frac{f_i}{N} \tag{17}$$

For bi-level thresholding, the pixels are divided into two classes which are denoted as C_1 and C_2. Then, the gray level probability distributions for the two classes are shown in Equation (18) and Equation (19):

$$C_1: \frac{p_1}{\omega_1(t)}, \dots, \frac{p_1}{\omega_1(t)} \tag{18}$$

and

$$C_2: \frac{p_{t+1}}{\omega_2(t)}, \frac{p_{t+2}}{\omega_2(t)}, \dots, \frac{p_L}{\omega_2(t)} \tag{19}$$

Where:

$$\omega_1(t) = \sum_{i=t+1}^{L} p_i \tag{20}$$

and

$$\omega_2(t) = \sum_{i=t+1}^{L} p_i \tag{21}$$

the means for classes C_1 and C_2 are also can be calculated as:

$$\mu_1 = \sum_{i=t+1}^{t} i\,\frac{p_i}{\omega_1}(t) \tag{22}$$

and

$$\mu_2 = \sum_{i=t+1}^{L} i\,\frac{p_i}{\omega_2}(t) \tag{23}$$

Let μ_T be the mean intensity for the whole image as shown in Equation (24) and Equation (25):

$$\omega_1\mu_1 + \omega_2\mu_2 = \mu_T \tag{24}$$

$$\omega_1 + \omega_2 = 1 \tag{25}$$

By using discriminant analysis, between-class variance of the thresholded image are defined by Otsu [13] as:

$$\sigma_B{}^2 = \omega_1(\mu_1 - \mu_T)^2 + \omega_2(\mu_2 - \mu_T)^2 \tag{26}$$

For bi-level thresholding, the between-class variance σ_B 2 is maximized when the optimal threshold t^* is chosen as verified by Otsu as shown in Equation (27):

$$t^* = \underset{1 \le t < L}{Arg\ Max}\,\{\sigma_B{}^2(t)\} \tag{27}$$

For multilevel thresholding of an image, the formula can be extended by assuming that there are M-1 thresholds, {$t1$, $t2$, ..., $tM-1$}, which can be divide with the original image into M classes, the optimal thresholds {$t1^*$, $t2^*$, ..., $tM-1^*$} are chosen by maximizing $\sigma_B{}^2$ as follows:

$$\{t_1{}^*, t_2{}^*, \dots, t_{M-1}{}^*\} = Arg\ Max\,\{\sigma_B{}^2(t_1, t_2, \dots, t_{M-1})\}, \tag{28}$$

$$1 \leq t_1 < \cdots < t_{M-1} < L$$

Where:

$$\sigma_B{}^2 = \sum_{k=1}^{M} \omega_k \, (\mu_k - \mu_T)^2, \tag{28}$$

with

$$\omega_k = \sum_{i \in Ck} p_i \tag{29}$$

$$\mu_k = \sum_{i \in Ck} i \, \frac{p_i}{\omega(k)} \tag{30}$$

The ω_k in Equation (29) is regarded as the zeroth-order cumulative moment of the k^{th} class C_k, and the numerator in Equation (30) is regarded as the first-order cumulative moment of the k^{th} class C_k, which shown in Equation (31):

$$\mu(k) = \sum_{i \in Ck} i \, p_i \tag{31}$$

4.0 RESULTS

For the Fuzzy C-Means (FCM) thresholding, the gray level is divided into three classes which are lower class, medium class and higher class. Then the clustering algorithm will automatically find the threshold value. The threshold value is being search between lower and middle classes. This is because there is more frequency at the lower gradient value. There is small different threshold value calculated by Fuzzy C-Means (FCM) and Otsu's thresholding. Figure 1 shows the gradient value of a sample. The green line indicates the Fuzzy C-Means (FCM) threshold value whereas the red line indicates the Otsu's threshold value that has been calculated.

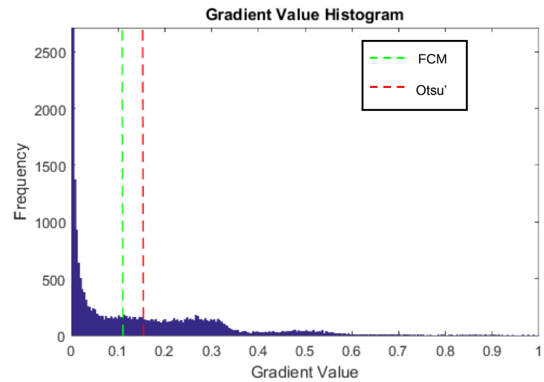

Figure 1 Gradient value Histogram.

The result of Fuzzy C-Means (FCM) and Otsu's segmentation are shown in Table 1. The segmentation accuracy is being evaluated by referring the manual segmentation pixels. There are three parts that are being evaluated which are the area overlap, false positive error and false negative error. Area overlap is the deform pixel which is correctly segmented, false positive error is the non-deform pixels is being segmented and false negative error is the deform pixels is not being segmented.

Table 2 shows the comparison of accuracy, false positive error and false negative error between two segmentation methods on three surface samples. By comparing the performance of Fuzzy C-Means (FCM) and Otsu's segmentation, the Fuzzy C-Means (FCM) segmentation accuracy gives higher accuracy then Otsu's method. The segmentation accuracy is low because at the pre-processing part, the border of the deformation area is being removed when correcting background illumination is being implemented.

Table 1 The segmentation results of FCM and Otsu's thresholding methods

	Samples Warp Image	Manual Segmentation	FCM	Otsu's
Car Door	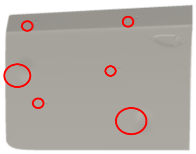		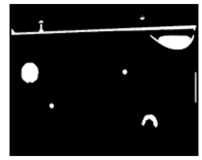	
Curve Surface	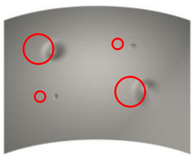	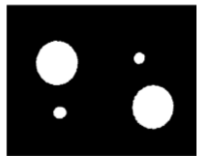	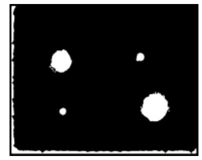	
Flat Surface	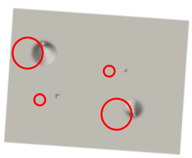	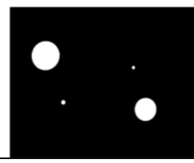	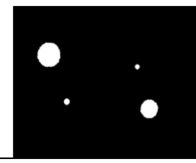	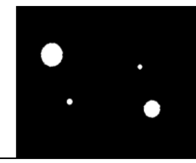

Table 2 Performance results between FCM and Otsu's methods on three surface samples

Methods	Samples	Accuracy	FPR	FNR	Sensitivity
FCM	**Car Door**	**19.09 %**	0.4343	**0.3748**	**0.3374**
	Curve Surface	**43.44 %**	0.3882	**0.1774**	**0.7100**
	Flat Surface	**41.87 %**	0.0000	**0.5813**	**0.4187**
Otsu's	**Car Door**	1.86 %	**0.2520**	0.7295	0.0248
	Curve Surface	31.38 %	**0.0196**	0.6667	0.3200
	Flat Surface	37.64 %	0.0000	0.6236	0.3764

5.0 CONCLUSION

In this paper, the Fuzzy C-Means (FCM) and Otsu's segmentation methods has been implemented to segment the deformation occur on the surfaces. Both methods have been compared with the manual segmentation to verify the accuracy. According to the results, Fuzzy C-Means (FCM) provides good segmentation results according to accuracy and sensitivity value, all the samples segmented by Fuzzy C-Means (FCM) method is higher than Otsu's method where the segmentation accuracy is 19.09 %, 43.44 % and 41.87 %. Although, the false positive rate (FPR) for Fuzzy C-Means (FCM) is higher than Otsu's method. Noted that the accuracy of three samples are below 50 %, this is because in pre-processing stage, the border of the deform area are also being removed. Therefore, the deform pixels has been decrease that cause the segmentation accuracy become lower. The enhancement can be made to increase the segmentation accuracy.

Acknowledgement

Appreciation to Universiti Teknikal Malaysia Melaka (UTeM) and Ministry of Higher Education (MOHE) for funding this work under the research grant ERGS/ 2013/ FKEKK/ TK02/ UTEM/03/05 E00021 and RACE/ F3/ TK8/ FKEKK/ F00251.

References

[1] Ghorai, S., Mukherjee, A., Gangadaran, M. and Dutta, P.K., 2013. Automatic Defect Detection On Hot-Rolled Flat Steel Products. *IEEE Transactions on*, *Instrumentation and Measurement*. 62(3): 612-621.

[2] Yogeswaran, A. and Payeur, P. 2012. 3D Surface Analysis for Automated Detection of Deformations on Automotive Body Panels. New Advances in Vehicular Technology and

Automotive Engineering, Chapter 12. *InTech.* ISBN: 978-953.

[3] Döring, C., Eichhorn, A., Girimonte, D. and Kruse, R. 2004. Improving Surface Detection For Quality Assessment Of Car Body Panels. *Mathware & Soft Computing.* 11(3).

[4] Chen, H. 2008. Automatic Dent Detection On Car Bodies.

[5] Jain, R., Kasturi, R. and Schunck, B. G. 1995. *Machine Vision*. New York: McGraw-Hill.

[6] Fisher, R., Perkins, S., Walker, A. and Wolfart, E. 2003. Gaussian Smoothing. *Hypermedia Image Processing Reference*.

[7] Amalorpavam, G., Naik, H. T., Kumari, J. and Suresha, M., 2013. Analysis of Digital Images Using Morphlogical Operations. *International Journal of Computer Science & Information Technology*. 5(1): 145.

[8] Sezgin, M., 2004. Survey Over Image Thresholding Techniques And Quantitative Performance Evaluation. *Journal of Electronic Imaging*. 13(1): 146-168.

[9] Bezdek, J. C., Ehrlich, R. and Full, W. 1984. FCM: The Fuzzy C-Means Clustering Algorithm. *Computers & Geosciences*. 10(2): 191-203.

[10] Suganya, R. and Shanthi, R. 2012. Fuzzy C-Means Algorithm-A Review. *International Journal of Scientific and Research Publications*. 2(11):1.

[11] Chordiya, M. A. R. and Bagal, S. B. 2015, January. Comparative Research of Clustering Algorithms for Prediction of Academic Performance of Students. In*International Journal of Engineering Research and Technology*. 4(01): (January-2015). ESRSA Publications.

[12] Liao, P. S., Chen, T. S. and Chung, P. C. 2001. A Fast Algorithm For Multilevel Thresholding. *Journal of Information Science and Engineering*. 17(5): 713-727.

[13] Otsu, N. 1975. A Threshold Selection Method From Gray-Level Histograms. *Automatica*. 11(285-296): 23-27.